5 × 5 25 Gbit/s WDM-MDM

DE GRUYTER J. Opt. Commun. 2015; 36(4): 327–333

Yousef Fazea* and Angela Amphawan

5 × 5 25 Gbit/s WDM-MDM

DOI 10.1515/joc-2014-0091
Received November 28, 2014; accepted February 12, 2015

Abstract: Wavelength-division multiplexed-passive optical network (WDM-PON) is a revolutionary high-capacity and scalable broadband access network. This paper capitalizes on Laguerre–Gaussian (LG) modes to reduce modal dispersion and increase data capacity. A data rate of 25 Gbit/s is attained for a multimode fiber link by multiplexing five LG modes on five wavelengths centered at 1,550.12 nm for a distance up to 800 m.

Keywords: wavelength-division multiplexing, mode division multiplexing, Laguerre–Gaussian modes

PACS. Fiber optics, Optical interconnects, Spatial multiplexing

1 Introduction

Wavelength-division multiplexed-passive optical network (WDM-PON) is a revolutionary high-capacity and scalable broadband access network [1]. The rapid growth of cloud computing, video streaming and mobile applications has led to an increase in bandwidth requirements [2–7]. Although a large number of 10 Gbit/s optical fiber networks have been laid by service providers [8], the increase in bandwidth demands have prompted mega data center operators to aggregate several 10 Gbit/s optical fibers together [9, 10].

A number of multiplexing techniques for increasing the data capacity through a single optical fiber have been proposed comprising wavelength [11, 12], polarization [13, 14], phase [14], amplitude [15, 16] and time dimensions [17, 18]. An elegant approach that has attracted significant attention is mode division multiplexing (MDM) [19], realized by combining or separating modes at the multiplexer and demultiplexer for transmitting independent data streams. Recent MDM demonstrations employ spatial light modulators [5, 21, 22], fiber gratings [23–28], digital signal processing algorithms [29–31], modal decomposition algorithms [32–34], adaptive optics [7, 35–38] and photonic crystal fiber [39].

The eminent factor restraining the bandwidth in MDM is the coupling of power from one axial direction to other directions. The coupling results in angular spread of light rays in each channel, which consequently governs the number of possible channels for a given crosstalk value and determines the pulse width in each channel. Thus far, relatively little consideration has been given to the separation of the modes for optimizing the bandwidth. This paper investigates the effect of separation of Laguerre–Gaussian (LG) modes on the channel performance.

This paper is organized as follows: Section 2 elucidates the MDM model for WDM-PON. Section 3 presents the results and discussion, and the conclusion of the paper is presented in Section 4.

2 WDM-based modal multiplexing

A WDM-based modal multiplexing model illustrated in Figure 1 is developed in OptSim 5.2 [40]. The model may be divided into three parts, namely, the transmitter, channel and the receiver. The transmitter consists of five vertical cavity emitting lasers (VCSELs) at five wavelengths, λ_1 to λ_5 between 1,546.92 nm and 1,553.33 nm, based on the ITU grid, separated by 1.6 nm with a center wavelength of 1,550.12 nm. The five VCSELs are driven by separate pseudorandom bit sequence (PRBS) electrical signals. The excitation of LG modes [40] for each VCSEL array is given in Tables 1 and 2 to evaluate the effect of separation modes in the azimuthal and radial directions, respectively. Non-return-to-zero modulation scheme is used. The power from each VCSEL is assumed to be emitted uniformly into 5 μm *x*-polarized LG beams. The five VCSEL signals are then combined using a wavelength division multiplexer. The signal is propagated through a multimode fiber between 200 and 800 m in length, in order to investigate the effects of the modes spacing between azimuthal and radial mode number on the channel performance in two scenarios. In Scenario 1, the

***Corresponding author: Yousef Fazea,** Integrated Optics Lab, School of Computing, Universiti Utara Malaysia, Sintok, Kedah, Malaysia, E-mail: yousef.a.fazea@ieee.org
Angela Amphawan, Integrated Optics Lab, School of Computing, Universiti Utara Malaysia, Sintok, Kedah, Malaysia; Research Laboratory of Electronics, Massachusetts Institute of Technology, Cambridge, MA, USA

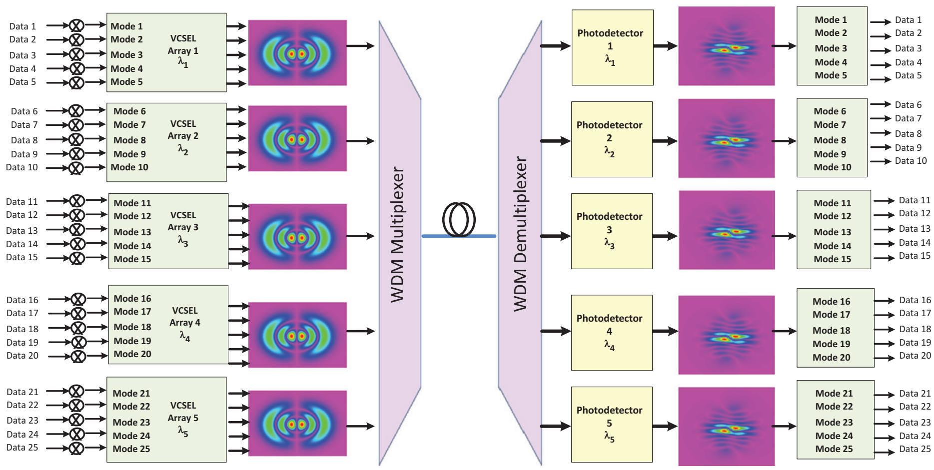

Figure 1: Laguerre–Gaussian mode division multiplexing model for evaluating the effect of spacing of radial mode number on transmission performance.

Table 1: Excitation of Laguerre–Gaussian modes for investigating the effect of separation between azimuthal mode numbers within VCSEL array on channel performance.

VCSEL array	Azimuthal mode number generated, l	Azimuthal mode number within VCSEL array	Radial mode number of VCSEL array, m
1	$l=1,2,3,4,5$	1	$m=2$
2	$l=1,3,5,7,9$	2	$m=2$
3	$l=1,4,7,10,13$	3	$m=2$
4	$l=1,5,9,13,17$	4	$m=2$
5	l$=1,6,12,16,21$	5	$m=2$

Table 2: Excitation of Laguerre–Gaussian modes for investigating the effect of separation between radial mode numbers within VCSEL Array.

VCSEL array	Radial mode number generated, m	Radial mode number within VCSEL array	Azimuthal mode number of VCSEL array, m
1	$m=1,2,3,4,5$	1	$l=2$
2	$m=1,3,5,7,9$	2	$l=2$
3	$m=1,4,7,10,13$	3	$l=2$
4	$m=1,5,9,13,17$	4	$l=2$
5	$m=1,6,12.16,21$	5	$l=2$

radial mode number m is maintained to $m=2$ while the azimuthal mode number l is varied at each run ranging from $\Delta l=1$, $\Delta l=2$, $\Delta l=3$, $\Delta l=4$ to $\Delta l=5$. In Scenario 2, the azimuthal mode number l is maintained to $l=2$ while the radial mode number m is varied at each run ranging from $\Delta m=1$, $\Delta m=2$, $\Delta m=3$, $\Delta m=4$ to $\Delta m=5$. At the receiver, the signal is then demultiplexed into five separate channels and the transverse modal field at each photodetector is examined. At each photodetector, the signal is analyzed using bit-error rate (BER) tester to observe the eye diagram and determine BER of each channel at different multimode fiber lengths.

3 Results and discussion

For evaluating of the effects of the azimuthal mode number l separations, the average BER per VCSEL array at various multimode fiber lengths are simulated in Figure 2. The BER for all variations of azimuthal mode number separation is acceptable except when $\Delta l=1$. Figure 3 shows the spatial transverse electric field for the center photodetector array with varying azimuthal mode number separations. As evident from Figure 3, the spatial transverse fields match the inherent modal fields of the multimode fiber more closely as Δl increases. For $\Delta l=1$, the close separation of the modes in the azimuthal direction significantly affects the accuracy of power coupling into the inherent mode. Thus, the spatial transverse electric field in Figure 3 confirms the BER curves in Figure 2.

Figure 4 shows a comparison of the eye diagrams illustrating the effect of azimuthal mode number separation for a multimode fiber length of 400 m whereby the radial mode number is maintained to 2. As the radial mode separation increases, the time deviation between propagation modes decreases and the eye opening widens. This is consistent with the BER curves in Figure 2 and the spatial transverse electric fields in Figure 3.

Figure 5 depicts the effect of the radial mode separation on the average BER per VCSEL for various multimode fiber lengths. For even values of $\Delta m=2$ and $\Delta m=4$, the

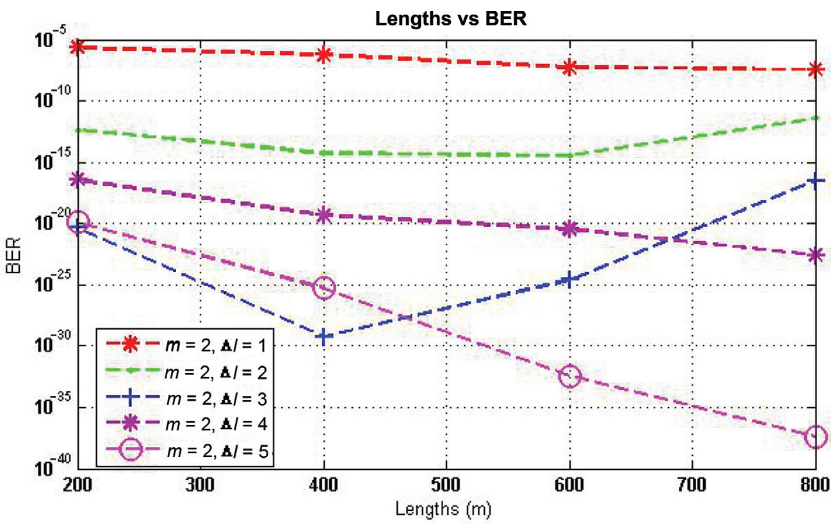

Figure 2: The effects of the azimuthal mode spacing for MMF length on bit error rare.

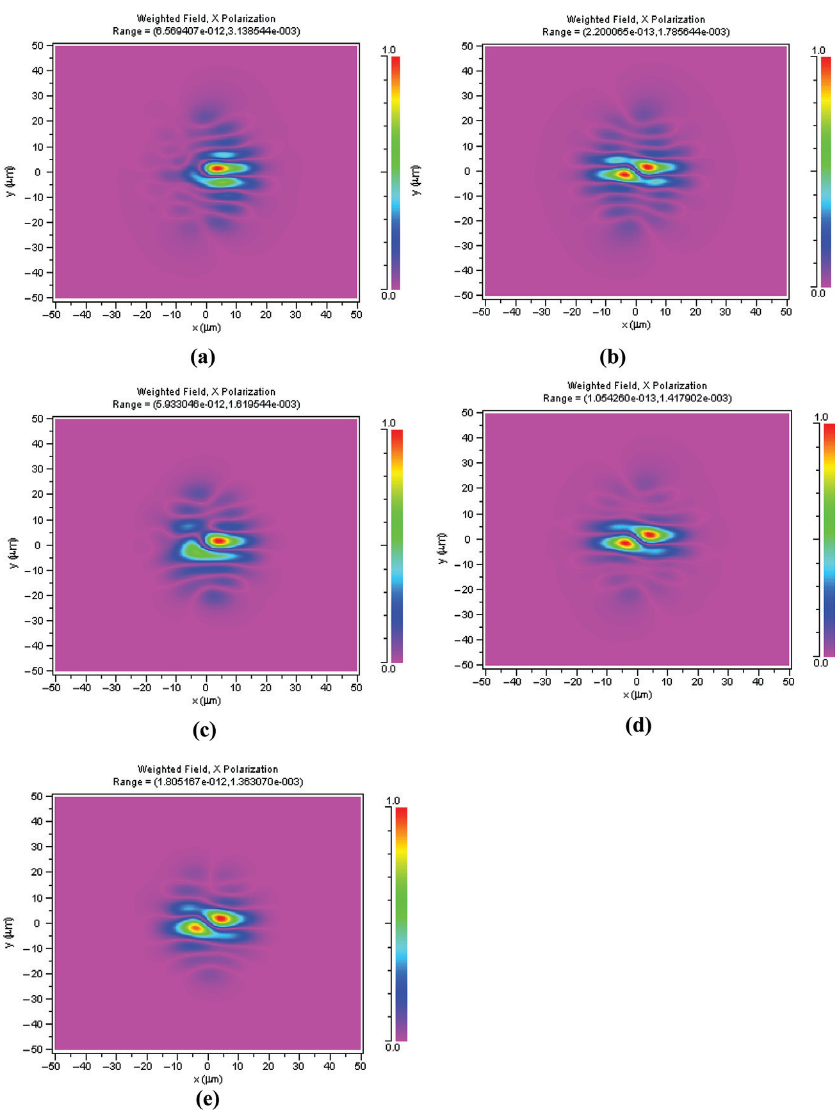

Figure 3: Transverse spatial electric field for center photodetector array after demultiplexer whereby the radial mode number $m = 2$ and the azimuthal mode number is varied at each run: (a) $\Delta l = 1$, (b) $\Delta l = 2$, (c) $\Delta l = 3$, (d) $\Delta l = 4$, (e) $\Delta l = 5$.

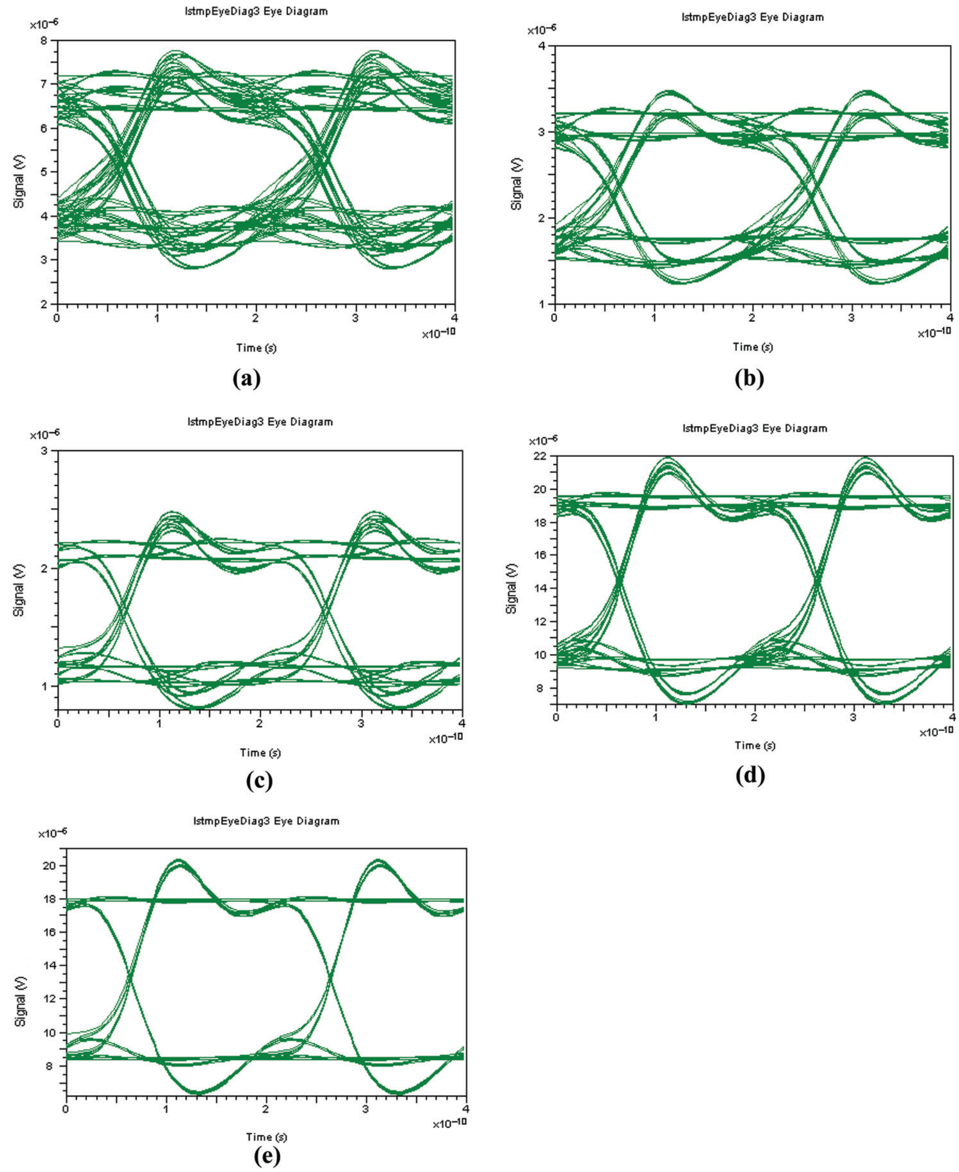

Figure 4: Eye diagram at λ = 1,550.12 nm showing the effect of azimuthal mode number separation at a length of 400 m whereby the radial mode number m = 2 and the azimuthal mode number is varied each run: (a) $\Delta l = 1$, (b) $\Delta l = 2$, (c) $\Delta l = 3$, (d) $\Delta l = 4$, (e) $\Delta l = 5$.

BER is better than odd-valued Δm as the polarities of the peaks of the spatial field cancel each other. For odd values $\Delta m = 3$ and $\Delta m = 5$, the polarities of the peaks of the spatial field are out of phase with one another. In addition, the BER is less than the acceptable BER range.

In Figure 6, the transverse spatial electric fields for center photodetector array after the demultiplexer for various radial mode number separations were analyzed. When the spacing of Δm is even, modes experience less modal dispersion while for odd values of Δm, modes experience high modal dispersion, consistent with results from Figure 5.

A comparison of eye diagrams showing the effect of radial mode number separations at a distance of 400 m is shown in Figure 7. Consistent with Figures 5 and 6, the time deviation is high for odd values of Δm and is low for even values of Δm.

4 Conclusion

In this paper, a 25-channel WDM-MDM model has been designed at a center wavelength of 1,550.12 nm in OptSim 5.2 multiplexing five LG modes on each VCSEL array on five different wavelengths. A transmission speed of 5 $\times$ 5 Gbit/s has been achieved, using five VCSEL arrays separated at 1.6 nm.

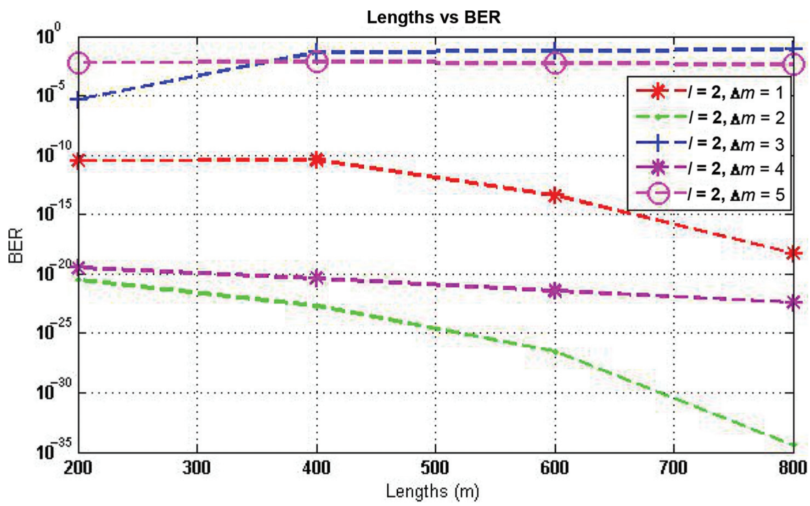

Figure 5: Effect of spacing of radial mode order and MMF length on bit error rate.

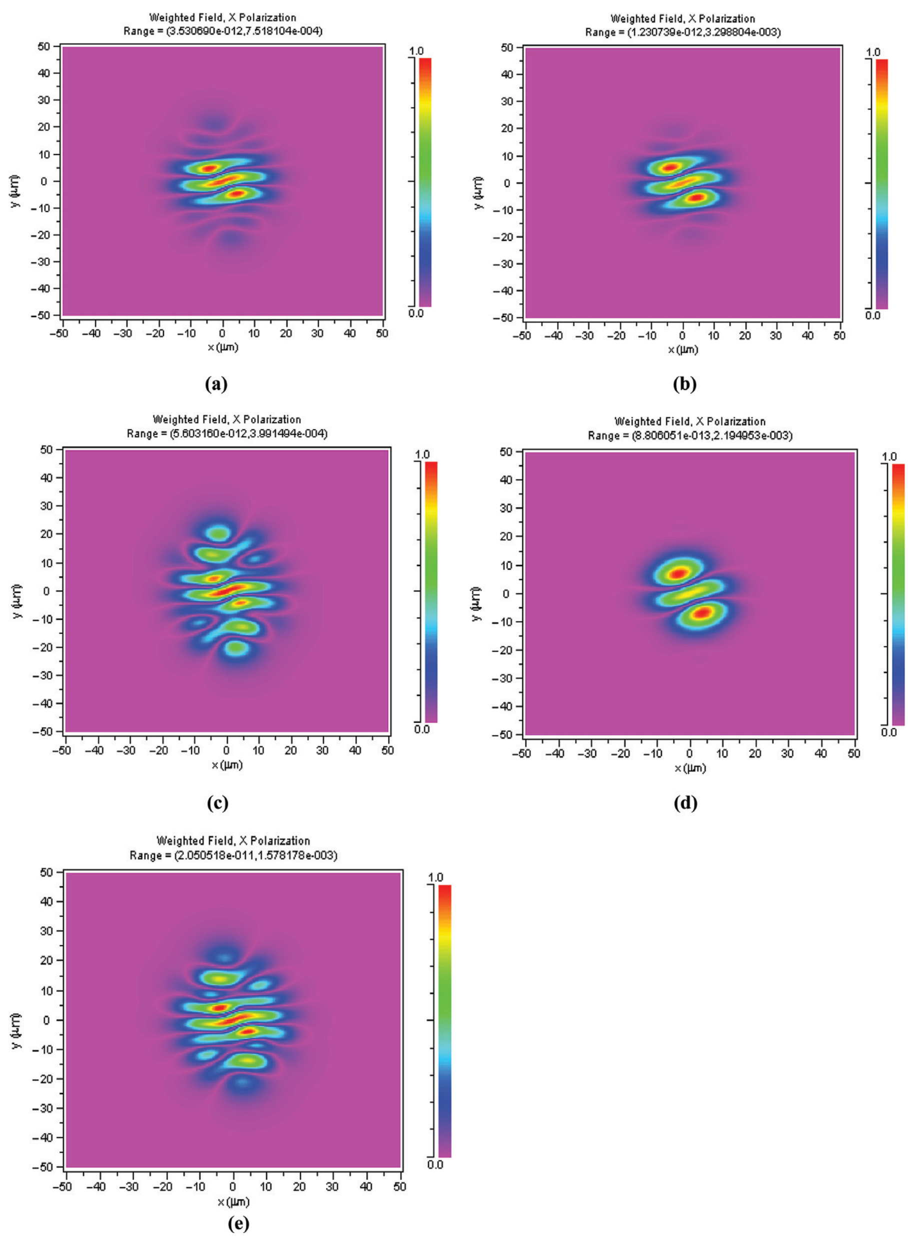

Figure 6: Transverse spatial electric field for center photodetector array at $\lambda = 1{,}550.12$ nm after demultiplexer for LG modes whereby the azimuthal mode number l maintained to 2 and the radial mode number fluctuates each run: (a) $\Delta m = 1$, (b) $\Delta m = 2$, (c) $\Delta m = 3$, (d) $\Delta m = 4$, (e) $\Delta m = 5$.

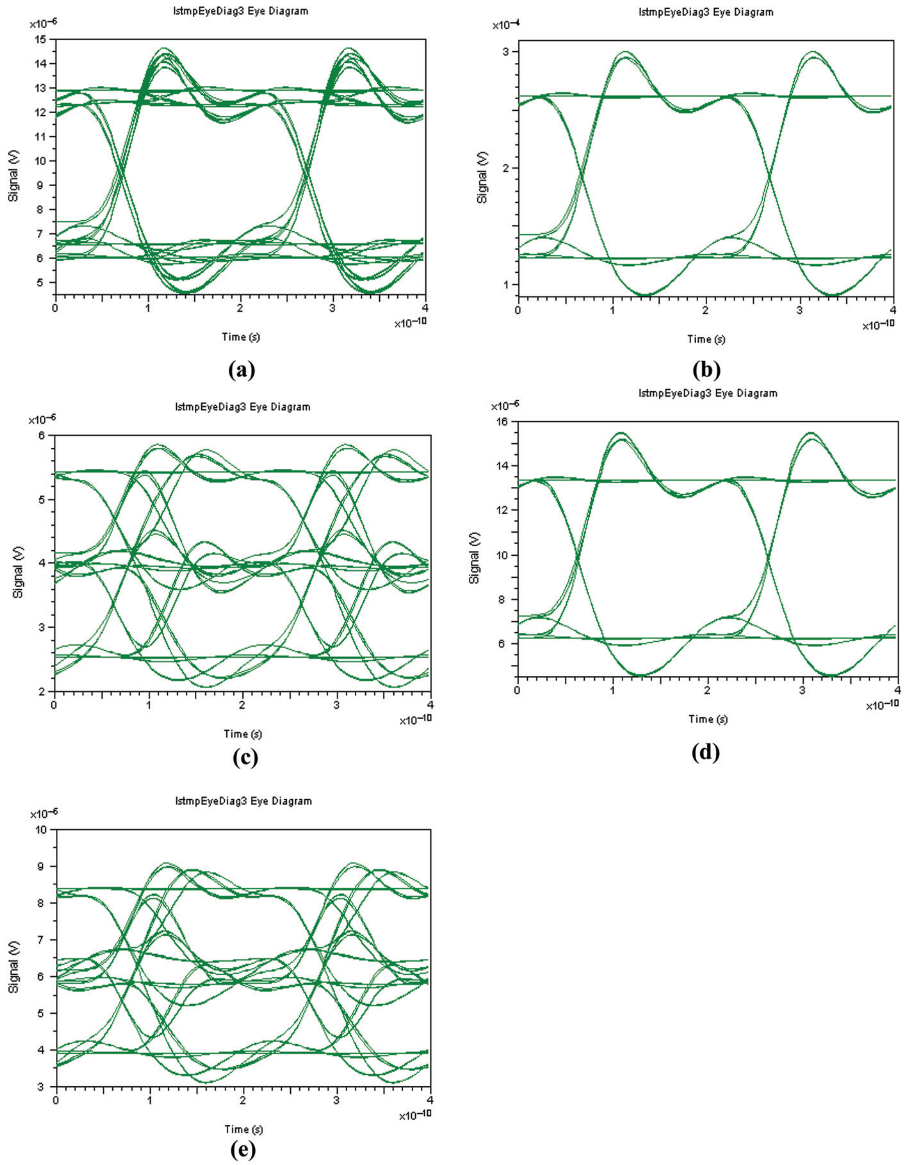

Figure 7: Eye diagram at $\lambda = 1{,}550.12$ nm showing the effect of radial mode number separation at a length of 400 m whereby the azimuthal mode number $l = 2$ and the radial mode number is varied at each run: (a) $\Delta m = 1$, (b) $\Delta m = 2$, (c) $\Delta m = 3$, (d) $\Delta m = 4$, (e) $\Delta m = 5$.

References

1. Zhuang W, Zhuang H, Zheng H, "Study on WDM-PON schemes." In: 2011 International Conference on Business Computing and Global In-formation, 2011.
2. Essiambre R, Kramer G, Winzer PJ, Foschini GJ, Goebel B. Capacity limits of optical fiber networks. J Lightwave Technol 2010;28:662–701.
3. Ryf R, Sierra A, Essiambre R-J, Randel S, Gnauck A, Bolle CA, et al. Mode-equalized distributed Raman amplification in 137-km few-mode fiber. In: European Conference and Exposition on Optical Communications, 2011, p. Th. 13. K. 5.
4. Inan B, Spinnler B, Ferreira F, Lobato Polo AP, Adhikari S, Sleiffer V, et al. Equalizer complexity of mode division multiplexed coherent receivers. In: Optical Fiber Communication Conference, 2012, p. OW3D. 4.
5. Amphawan A. Holographic mode-selective launch for bandwidth enhancement in multimode fiber. Opt Exp 2011;19:9056–65.
6. Stepniak G, Maksymiuk L, Siuzdak J. Increasing multimode fiber transmission capacity by mode selective spatial light phase modulation. In: 36th European Conference on Optical Communications, 2010.
7. Carpenter J, Wilkinson TD. Precise modal excitation in multimode fibre for control of modal dispersion and mode-group division multiplexing. In: European Conference and Exposition on Optical Communications, 2011, p. We. 10. P1. 62.
8. Cheng N, Zhenxing L, Liu S, Effenberger F. Gain-clamped semiconductor optical amplifiers for reach extension of coexisted GPON and XG-PON. In: National Fiber Optic Engineers Conference, 2011, p. NTuD7.
9. Choi J, Yoo M, Mukherjee B. Efficient video-on-demand streaming for broadband access networks. J Opt Commun Networking 2010;2:38–50.

10. Casier K, Verbrugge S, Meersman R, Colle D, Pickavet M, Demeester P. A clear and balanced view on FTTH deployment costs. In: Proceedings of FITCE Congress, 2008, p. 109.
11. Urata R, Lam C, Liu H, Johnson C. High performance, low cost, colorless ONU for WDM-PON. In: National Fiber Optic Engineers Conference, 2012, p. NTh3E. 4.
12. Bobrovs V, Spolitis S, Ivanovs G. Comparison of chromatic dispersion compensation techniques for WDM-PON solution. In: 2012 2nd Baltic Congress on Future Internet Communications (BCFIC), 2012, pp. 64–67.
13. Hanzawa N, Saitoh K, Sakamoto T, Matsui T, Tomita S, Koshiba M. Demonstration of mode-division multiplexing transmission over 10 km two-mode fiber with mode coupler. In: Optical Fiber Communication Conference and Exposition (OFC/NFOEC), 2011 and the National Fiber Optic Engineers Conference, 2011, pp. 1–3.
14. Salsi M, Koebele C, Sperti D, Tran P, Brindel P, Mardoyan H, et al. Transmission at 2x100Gbit/s, over two modes of 40km-long prototype few-mode fiber, using LCOS based mode multiplexer and demultiplexer. In: National Fiber Optic Engineers Conference, 2011, p. PDPB9.
15. Al-Khafaji H, Aljunid S, Amphawan A, Fadhil H. Improving spectral efficiency of SAC-OCDMA systems by SPD scheme. IEICE Electron Exp 2012;9:1829–34.
16. Al-Khafaji H, Aljunid S, Amphawan A, Fadhil H. SOA/SPD-based incoherent SAC-OCDMA system at 9 × 5 Gbit/s. IEICE Electron Exp 2013;10:p. 20130044.
17. Harstead E, Sharpe R. Future fiber-to-the-home bandwidth demands favor time division multiplexing passive optical networks. Commun Mag IEEE 2012;50:218–23.
18. Kusakabe T, Kurakake T, Oyamada K, Fujita Y. Time-division multiplexing method for transmitting digital broadcasts over FTTH. IEICE Commun Exp 2013;2:428–34.
19. Al Amin A, Li A, Chen X, Shieh W. Spatial mode division multiplexing for overcoming capacity barrier of optical fibers. In: 2011 16th Optoelectronics and Communications Conference (OECC), 2011, pp. 415–6.
20. Amphawan A. Binary encoded computer generated holograms for temporal phase shifting. Opt Exp 2011;19:23085–96.
21. Amphawan A. Binary spatial amplitude modulation of continuous transverse modal electric field using a single lens for mode selectivity in multimode fiber. J Mod Opt 2012;59:460–9.
22. Amphawan A, O'Brien D. Holographic mode field generation for a multimode fiber channel. In: Presented at the Proc. IEEE International Conference on Photonics 2010 (ICP2010), Langkawi, 2010.
23. Hanzawa N, Saitoh K, Sakamoto T, Matsui T, Tomita S, Koshiba M. Mode-division multiplexed transmission with fiber mode couplers. In: Optical Fiber Communication Conference, 2012, p. OW1D. 4.
24. Al Amin A, Li A, Chen S, Chen X, Gao G, Shieh W. Dual-LP 11 mode 4x4 MIMO-OFDM transmission over a two-mode fiber. Opt Exp 2011;19:16672–9.
25. Giles I, Obeysekara A, Chen R, Giles D, Poletti F, Richardson D. Fiber LPG mode converters and mode selection technique for multimode SDM. Photonics Technol Lett IEEE 2012;24: 1922–5.
26. Fang L, Jia H. Mode add/drop multiplexers of LP 02 and LP 03 modes with two parallel combinative long-period fiber gratings. Opt Exp 2014;22:11488–97.
27. Li A, Amin AA, Chen X, Chen S, Gao G, Shieh W. Reception of dual-spatial-mode CO-OFDM signal over a two-mode fiber. Lightwave Technol J 2012;30:634–40.
28. Ung B, Vaity P, Rusch L, Messaddeq Y, LaRochelle S. Characterization of optical fibers supporting OAM states using fiber Bragg gratings. In: CLEO: Science and Innovations, 2014, p. SM2N. 4.
29. Panicker RA, Kahn JM. Algorithms for compensation of multimode fiber dispersion using adaptive optics. J Lightwave Technol 2009;27:5790–9.
30. Panicker RA, Lau AP, Wilde JP, Kahn JM. Experimental comparison of adaptive optics algorithms in 10-gbit/s multimode fiber systems. J Lightwave Technol 2009;27:5783–9.
31. Shemirani MB, Wilde JP, Kahn JM. Adaptive compensation of multimode fiber dispersion by control of launched amplitude, phase, and polarization. J Lightwave Technol 2010;28:2627–39.
32. Kaiser T, Flamm D, DuparrÚ M. Complete modal decomposition for optical fibers using CGH-based correlation filters. Opt Exp 2009;17:9347–56.
33. Amphawan A, O'Brien D. Modal decomposition of output field for holographic mode field generation in a multimode fiber channel. In: 2010 International Conference on Photonics (ICP), 2010, pp. 1–5.
34. Jiang Z, Marciante JR. Precise modal decomposition in multimode optical fibers by maximizing the sum of modal power weights. In: Frontiers in Optics, 2008, p. FMD4.
35. Amphawan A, Mishra V, Nisar K, Nedniyom B. Real-time holographic backlighting positioning sensor for enhanced power coupling efficiency into selective launches in multimode fiber. J Mod Opt 2012;50:1745–52.
36. Carpenter J, Wilkinson TD. Adaptive enhancement of multimode fibre bandwidth by twin-spot offset launch. In: Conference on Lasers and Electro-Optics/Pacific Rim, 2011, p. C413.
37. Carpenter J, Thomsen BC, Wilkinson TD. Degenerate mode-group division multiplexing. J Lightwave Technol 2012;30:3946–52.
38. Carpenter J, Wilkinson TD. Characterization of multimode fiber by selective mode excitation. J Lightwave Technol 2012;30:1386–92.
39. Amphawan A, Samman NM, Nedniyom B. Selective excitation of LP01 mode in multimode fiber using solid-core photonic crystal fiber. J Mod Opt 2013;60:1675–83.
40. Amphawan A, Alabdalleh WA. Simulation of properties of the transverse modal electric field of an infinite parabolic multimode fiber. Microwave Opt Lett 2012;54:1362–5.